AIMS Biophysics

AIMS Biophysics, 7(3): 189–203.
DOI: 10.3934/biophy.2020015
Received: 02 May 2020
Accepted: 15 June 2020
Published: 18 June 2020

http://www.aimspress.com/journal/biophysics

Research article

Calorimetry and FTIR reveal the ability of URG7 protein to modify the aggregation state of both cell lysate and amylogenic α-synuclein

Jany Dandurand[1,*], Angela Ostuni[2,*], Maria Francesca Armentano[2], Maria Antonietta Crudele[2], Vincenza Dolce[3], Federica Marra[3], Valérie Samouillan[1] and Faustino Bisaccia[2]

[1] CIRIMAT, Physique des Polymères, Université Paul Sabatier, Toulouse, France
[2] Department of Sciences, University of Basilicata, Potenza, Italy
[3] Department of Pharmacy, Health and Nutritional Sciences, University of Calabria, Italy

*** Correspondence:** Email: jany.lods@univ-tlse3.fr, angela.ostuni@unibas.it; Tel: + 33561556816.

Abstract: Differential scanning calorimetry and FITR analyses allowed to investigate the role of URG7 (up-regulated gene clone 7) protein involved in the development of hepatocellular carcinoma induced by hepatitis B virus infection, on the physical structure both of lysates of human hepatoblastoma cells (HepG2) stressed with tunicamycin and α-synuclein, one of the proteins associated with neurogenerative diseases. The protein-water interfacial region was identified and correlated with protein structure. DSC results confirm through the interfacial water behavior that URG7 is able to act in two ways: it maintains the interfacial water stability and controls the mobile fraction level, thereby the flexibility and the protein folding. The mobile water phase increases strongly for cells exposed to α-synuclein, demonstrating an important influence on water hydration. FTIR results evidenced an increase of about 30% of cross β structures in cells exposed to α-synuclein, associated with aggregated proteins. In stress conditions, URG7 was able to maintain the same fraction of mobile water as untreated cells. URG7 was able to restore the water reorientation ability around the complex lysate system and reduced abnormal protein folding.

Keywords: URG7; Differential Scanning Calorimetry; physical structure; interfacial water; protein aggregation; synuclein

1. Introduction

URG7 (up-regulated gene clone 7) is a protein transactivated by the hepatitis B antigen X, localized into endoplasmic reticulum [1–4] and involved in the development of hepatocellular

carcinoma induced by hepatitis B virus infection [5]. It has been reported that URG7 inhibits TNF alpha-mediated apoptosis by blocking one or more caspases in the apoptotic pathway and by activating the phosphoinositide 3-kinase and β-catenin [6,7], thus suggesting that URG7 helps to protect hepatocytes during chronic hepatitis B virus infection. Previously, we reported that, in endoplasmic reticulum (ER)-stressed cells, URG7 is able to modulate the expression of Unfolded Protein Response (UPR) markers towards survival outcomes, up-regulating GRP78 protein and down-regulating the pro-apoptotic protein CHOP [8]. URG7 reduces the ER stress by decreasing the amount of unfolded proteins and by increasing both the total protein ubiquitination and the AKT activation. Considering the accumulation of misfolded proteins in HBV infected cells, is clear its role as an anti-apoptotic protein. Nevertheless it is unclear whether the observed effects on the tunicamycin stressed cells are the result of AKT activation or URG7 is by itself able to modify the protein folding and aggregation directly interacting with unfolded proteins.

In order to shed light on the mechanism by which URG7 could modulate protein folding, in vitro experiments were carried out to evaluate the protein aggregation of lysates of HepG2 cells previously transfected with URG7 gene and stressed with tunicamycin or treated with a specific URG7-derived peptide identified as 75–99 URG7-peptide [9]. Moreover, the effect of URG7-derived peptide was also checked on α-synuclein, the major component of abnormal aggregates in neurodegenerative disorders [10–12].

Structural stability and flexibility of proteins are closely connected to their molecular and supramolecular organization as well as and their surface hydration; in this sense, the use of techniques devoted to structural and thermodynamic characterization of proteins in their cellular environment appear highly adequate to contribute to a better knowledge of biological activity of proteins and peptides sequences. Thermal and vibrational analyses constitute an efficient approach to obtain additional parameters on biological data [2,3,8]. Differential scanning calorimetry is a useful technique to study protein folding and stability [13], protein denaturation in biological compounds [14], aggregation and self-assembly of proteins and peptides.

2. Materials and methods

2.1. Cell culture and treatments

Human hepatoblastoma cells (HepG2) were maintained at 37 ℃, in a humidified 5% CO_2 atmosphere, in DMEM containing 4.5 g/L glucose, supplemented with 10% fetal FBS, 2 mM L-glutamine, 100 U/mL penicillin and 100 μg/mL streptomycin. In all the experiments, after trypsinization, cells were lysed in RIPA buffer (50 mM Tris-HCl pH 8, 150 mM NaCl, 1% Igepal, 0.2% SDS, 1% sodium deoxycholate, 1% protease inhibitor cocktail). In some experiments, the 75–99 URG7-peptide (417 μM), a scrambled peptide (P2) (see paragraph 2.3.) or α-synuclein (250 μM) (see paragraph 2.4.) were then added to the lysates, which were subsequently frozen and finally freeze-dried. Where indicated, cells were treated with the antibiotic tunicamycin (3 μg/ml final concentration) for 15 h to induce ER-stress.

2.2. URG7 cell transfection

The expression of URG7 protein was determined in HepG2 cell line by transient transfection of the pcDNA3/URG7flag fusion plasmid (defined as URG7), using TransIT-2020 Transfection

Reagent (MIRUS), according to the manufacturer's instructions, as previously described [8]. The plasmid construct were allowed to express URG7 for 33 h before adding the antibiotic tunicamycin for additional 15 h to induce ER-stress. The empty vector pcDNA3 (mock) was used as negative control.

2.3. URG7-peptide synthesis

Peptide corresponding to the last 25 aminoacids of the URG7 protein (75-99 URG7-peptide), was synthesized on a Pioneer PerSeptive Biosystem synthesizer by the solid-phase method using Fmoc chemistry. Coupling reagents (0.5 M PyBop/DMF and 1.0 M DIPEA/DMF) were used with a four-fold excess of amino acid. Trifluoroacetic acid (TFA)/H_2O/thioanisole/phenol/ethanedithiol (88%, 3%, 3%, 4%, 2%) mixture was used for the deprotection and cleavage of the peptide.

Crude peptide was precipitated in cold diethyl ether, then lyophilized, and finally purified using reverse-phase HPLC on a Phenomenex C18 column (2.5 * 300 mm, 5 μm particles) with a gradient of acetonitrile/water in 0.1% TFA. The molecular mass of the peptide was confirmed by mass spectroscopy. Protein concentration was determined by measuring the optical absorbance at 280 nm using 5500 $M^{-1}cm^{-1}$ as the extinction coefficient calculated from the amino acid composition.

The same synthesis and purification procedures were used for the scrambled peptide (P2).

2.4. Expression and purification of α-synuclein

The Escherichia coli strain BL21(DE3) (Stratagene, La Jolla, CA, USA) was transformed with the expression vector pMW7 containing the α−synuclein (Isoform 1, P37840-1) gene in fusion with a histidine tag**.** A single colony was used to inoculate, overnight at 37 ℃ with shaking in Luria broth containing 100 μg/mL ampicillin. The o/n culture was diluted 1: 25 and the expression of α-synuclein was induced at the exponential phase of growth by the addition of isopropylthiogalactoside (IPTG, 1 mM). The cells were collected by centrifugation 4 h after induction, sonicate in Tris 10 mM, EDTA 1 mM, pH 7 and then recovered by centrifugation. Proteins were analyzed by SDS-PAGE gel; western blot analysis was performed using αSyn monoclonal antibody clone 4D6 (1: 10,000; Biolegend) and horseradish peroxidase-conjugated anti-mouse IgG. Recombinant α-synuclein was purified from soluble protein fraction after sonication by affinity chromatography with HisTrap HP (GE Healthcare) [15]; its concentration was determined spectrophotometrically using an extinction coefficient of 5960 $M^{-1}cm^{-1}$ at 280 nm.

2.5. Calorimetric analysis

Calorimetric analyses were performed using a DSC Pyris calorimeter (Perkin Elmer, Waltham, MA, USA). The calorimeter was calibrated using cyclohexane and indium as standards, resulting in a temperature accuracy of 0.1 ℃ and an enthalpy accuracy of 0.2 J/g.

High resolution thermograms were recorded by steps of 0.01 ℃. Samples solutions were prepared by adding 50 μL ultrapure water to lyophilized cell lysates, leading to a concentration of 4 mg/mL.

All the samples (15 μL) were sealed in hermetic aluminum pans and an empty pan was used as reference. An isotherm at 37 ℃ for 1 hour was performed to equilibrate the solutions and to bring to the fore eventual self-assembling processes. Next, samples were cooling to −100 ℃ at 10 ℃/min,

then the thermograms were recorded during the heating at 10 ℃/min until 80 ℃. The 10 ℃/min cooling and heating rates were chosen to obtain well-defined and reproducible results. Three replicates were performed for each sample.

Information about structural and dynamic changes can be deduced from the amount of heat absorbed or emitted by the sample to controlled temperature rate. Quantification of the different types of water molecules had been previously described [16].

2.6. FTIR-ATR spectra

FTIR-ATR spectra were performed using a Nicolet 5700 (THERMO FISHER SCIENTIFIC, Waltham, MA) equipped in ATR accessory (Smart Orbit with a type IIA diamond crystal, refractive index 2.4) with a KBr beam splitter and an MCT/B detector.

1 μL of solution was dropped in the ATR device and allowed to dry for 1 hour. Measurements on the resulting dried films were recorded over the region of 4000–450 cm^{-1} with a spectral resolution of 2 cm^{-1} and 32 accumulations. Background spectra were recorded before each experiment and subtracted from the sample's spectra.Three replicates were performed for each sample.

Data were collected using Omnic 8.0 (THERMO FISHER SCIENTIFIC, Waltham, MA). Then spectra were baseline corrected, smoothed (13 points Savitzky-Golay). Two distinct normalizations were performed. Spectra were normalized to the 1465 cm^{-1} peak using the minimum-maximum normalization to a better comparison between cells lysates and buffer preparations. The classical Amide I area normalization was performed to compare with each other only cells lysates spectra in the Amide I region. In order to quantify the evolution of the secondary structures amount in the different cellular preparations, a decomposition of the Amide I was performed using the Peak Resolve function in the Omnic 8.0 Software. In the curve fitting procedure, the location of the peaks was computed using the second derivative method and a combination of Gaussian-Lorentzian peaks shape was used for all the peaks. Second derivatives and Fourier-Self-Deconvolution (FSD) were also used to enhance the chemical information present in overlapping infrared absorption bands.

3. Results

3.1. Differential Scanning Calorimetry

Human hepatoma cell line, HepG2 was previously used as a cell model to study ABCC6 gene encoding a membrane protein named MRP6, which presents high homology with URG7 sharing the first 74 amino acids [17–20]; in addition, α-synuclein, a small protein, with a high conformational plasticity [12], have been chosen to evaluate the potential of URG7 as a folding modifier.

Three series of *in vitro* experiments were performed to evaluate the effects of tunicamycin or α-synuclein on control cells, URG7 transfected cells or subsequently URG7 treated cells.

In the first case, DSC measurements were carried out in order to investigate the specific thermal answer and the physical structure of HepG2 and HepG2-URG7 transfected cells lysates. At low temperature, DSC heating curves of cells lysates were characterized by two endothermic peaks (Figure 1). The specific [−30, −20 ℃] zone could be particularly studied in term of eutectic melting, while in inset was reported the [−10, 15 ℃] zone corresponding to the melting of frozen water, or melting of primary ice [16]. A similar feature is often reported for highly hydrated biological samples [21,22]. The characteristics of these two main endotherms were reported in Table 1 for the cellular samples.

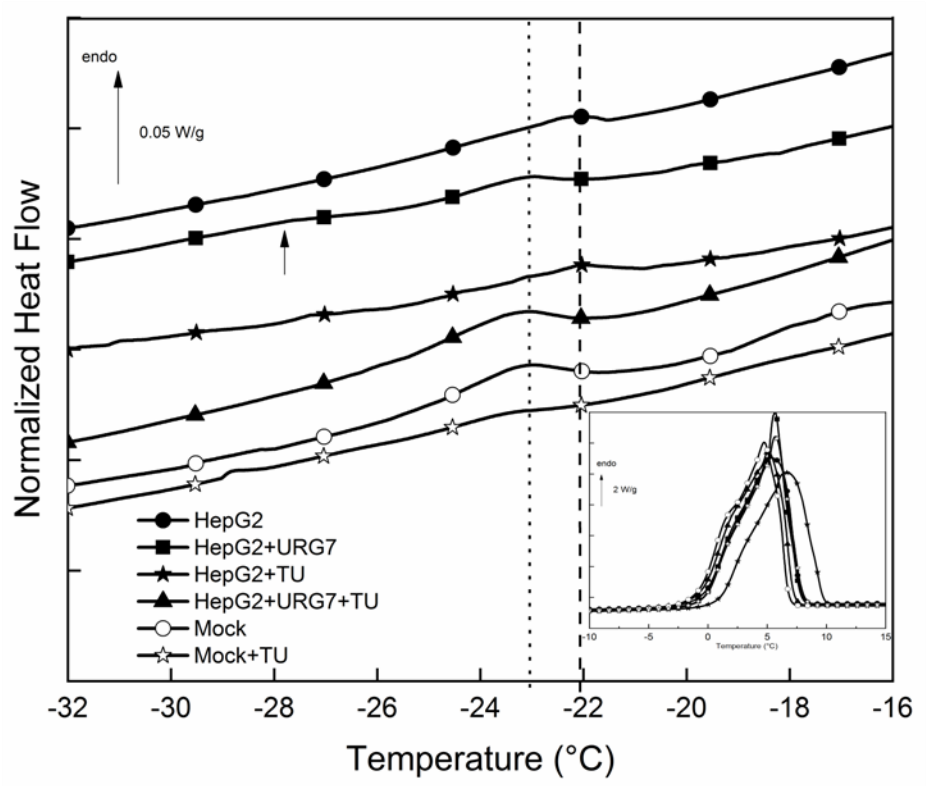

Figure 1. DSC heating curves of control and URG7-transfected cells lysates, untreated and TU treated, enlargement of the interest zone. In the inset the [−10, 15 ℃] zone is shown.

Table 1. Characteristic parameters of the main endotherms in DSC thermograms.

	Samples	Eutectic		Primary ice	
		T (℃)	ΔH (J/g)	T (℃)	ΔH (J/g)
TU Transfected cells	HepG2	-22.4	0.08	5.3	287
	HepG2 TU	-22.1	0.02	6.7	273
	HepG2 URG7	-23.1	0.05	5.7	296
	HepG2 TU URG7	-23.5	0.2	5.1	289
TU Treated Cells	HepG2	-21.5	3.5	4.6	271
	HepG2 TU	-19	1.5	8.2	269
	HepG2 URG7	-22.2	2.5	3 peaks	266
	HepG2 TU URG7	-20.5	1.1	5.5	280
SYN Treated cells	HepG2	-21.6	0.02	6.2	262
	HepG2 SYN	-22.3	0.9	4.2	265
	HepG2 URG7	----------	---------	4.9	265
	HepG2 SYN URG7	----------	---------	5.2	256

HepG2 cell lysates presented an endothermic event at −22 ℃. With tunicamycin stress treatment (TU) we noted a decrease of the eutectic melting enthalpy, indicative of reduced fraction water involved. In lysates of URG7 transfected cells the peak was shifted toward low temperature and a second minor event was detected at −28 ℃; the decrease of this peak temperature with URG7

transfection can be interpreted as a destabilization of this eutectic. The multiplicity of the peaks evidences a more complex water structure surrounding the sample. The eutectic enthalpy in TU stressed URG7 transfected HepG2 cells strongly increases. While TU stressed cells leads to a decrease of eutectic fraction, URG7 transfection counteracts the effects of TU.

Mock cells transfected with an empty vector were used to control transfection effects: it was evidenced via thermal parameters that TU had a similar effect on these cells.

In the second case, DSC measurements were carried out on HepG2 cells or HepG2 cells treated with tunicamycin (HepG2+TU) then lysated and finally treated with URG7-peptide or a scrambled peptide (Figure 2). As for the first series of DSC measurements, we could note two endothermic peaks for each curve (parameters in Table 1). TU treatment induced an important shift toward high temperature of this peak, fingerprints of a stabilized structure, and a decrease of the associated melting enthalpy. HepG2 cell lysates treated with P2 peptide was used to control the specificity of peptide effect; P2 induced a decrease of peak area (not reported on Table), but unmodified the melting temperature. The eutectic peak was shifted toward low temperature when the URG7-peptide was added in the control cells lysates, indicating a destabilization effect. Finally, in tunicamycin stressed HepG2 cell lysates treated with URG7-peptide, the eutectic temperature was intermediate between URG7 and control cells ones, but the enthalpy remained lower. URG7-peptide acted to preserve the thermal behavior of HepG2 lysates eutectic water but was unable to maintain its fraction.

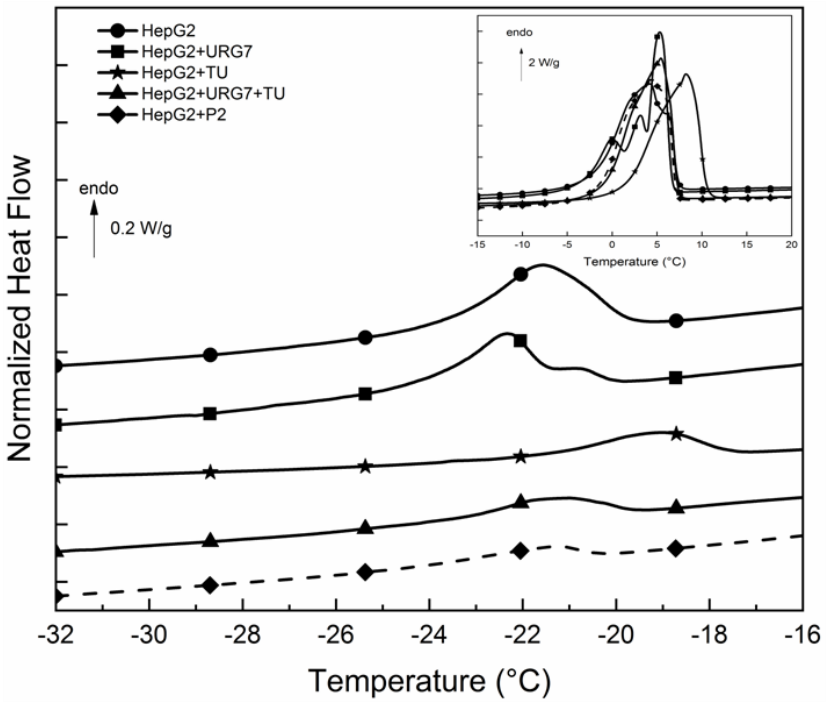

Figure 2. DSC curves of cell lysates, untreated and treated by TU and/or URG7, enlargement of the interest zone**.** HepG2 or HepG2 treated with Tunicamycin (HepG2+TU) were lysed. Then URG7-peptide (HepG2+URG7) or scrambled peptide (HepG2+P2) were added. In the inset a comparison of DSC heating thermograms in the [−15, 20 ℃] zone is shown.

Finally, similar DSC experiments have been conducted on HepG2 cell lysates treated with

URG7-peptide and Synuclein (SYN), associated with neurodegenerative diseases [10,23] (Figure 3 and Table 1). As a control we used lysis buffer alone. Below 0 ℃, the comparison of the calorimetric signature of the different samples showed a very weak eutectic event for HepG2 cells, which completely vanished in HepG2 cells treated with URG7. This eutectic melting was enhanced in HepG2 cell lysates treated with SYN, indicative of an important water fraction involved. This peak did not occur in HepG2 cell lysates treated with both SYN and URG7-peptide, tending to prove that URG7-peptide inhibits or modifies interfacial hydration structure.

Pure buffer curve showed a weak eutectic peak, shifted to low temperature by addition of SYN, and vanishing with addition of URG7. On the contrary, buffer URG7+SYN exhibited a broad eutectic melting.

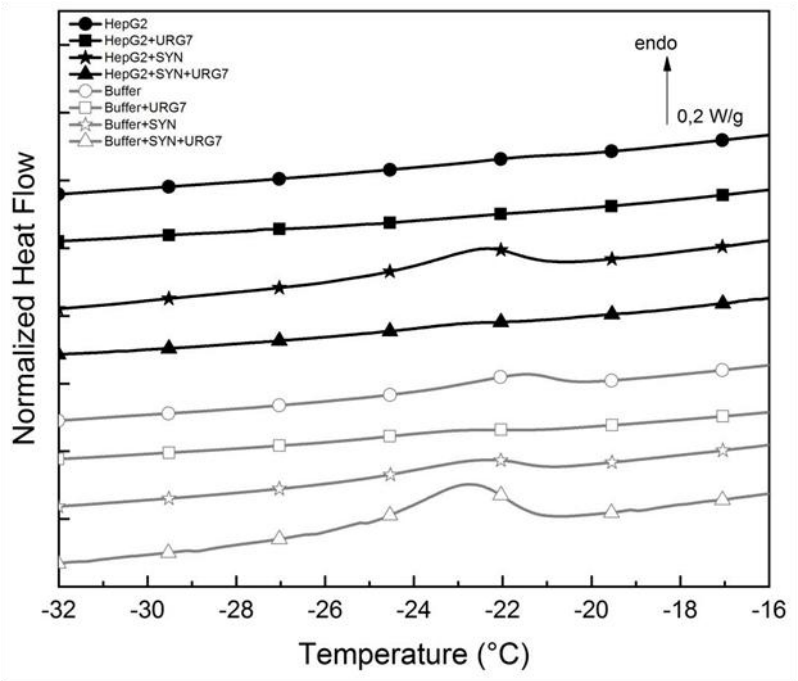

Figure 3. DSC curves of HepG2 cell lysates treated with URG7-peptide (HepG2+URG7), Synuclein (HepG2+SYN), or URG7-peptide and Synuclein (HepG2+SYN+URG7) (black line). As a control URG7-peptide, Synuclein or both were added to lysis buffer (grey line), enlargement of the interest zone.

3.2. FTIR spectroscopy

FTIR spectroscopy made on the third series of samples previously described provided information on the structural conformations and allowed to monitor their evolution with the different treatments. The raw FTIR spectrum of the four cellular preparations (those considered in Figure 3) is presented in Figure 4.

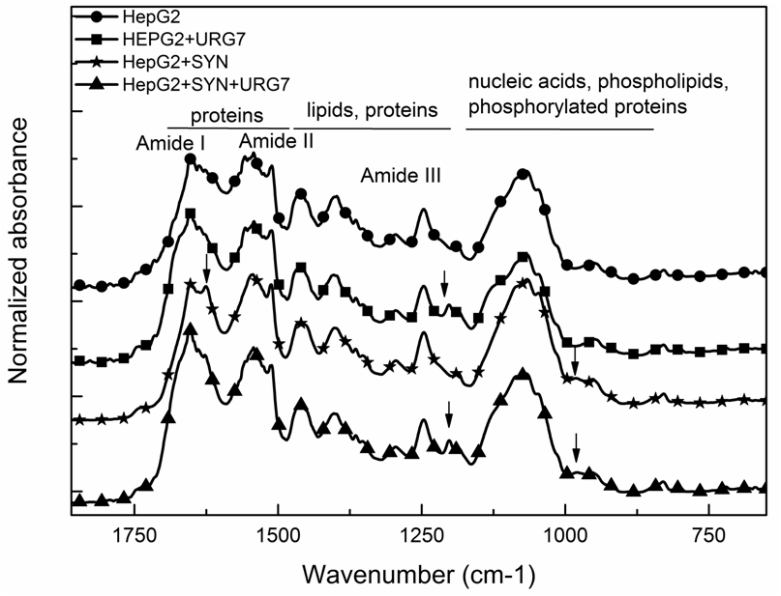

Figure 4. Raw FTIR spectra of cellular dried films in the 1800–700 cm^{-1} zone.

As indicated on Figure 4, the classical absorption bands of proteins, lipids, phospholipids and nucleic acids are present in these spectra [24]. Some important differences are detectable on these spectra and pointed by arrows. As seen in the enlargement of the 1230–1150 cm^{-1} zone (Figure 5), the band at 1204 cm^{-1} is only detectable in URG7 treated cellular preparations and associated buffers. It can be unambiguously attributed to the specific answer of URG7-peptide in these preparations.

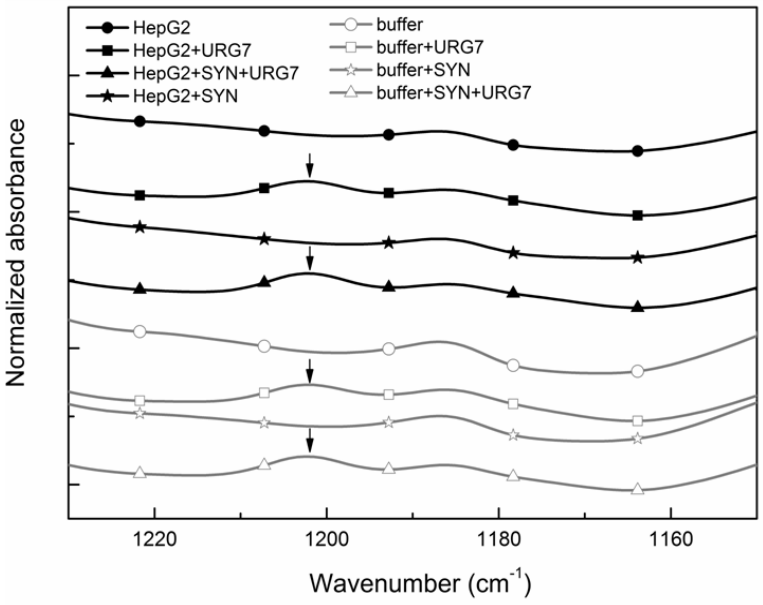

Figure 5. Raw FTIR spectra of cellular dried films and buffer preparations in the 1230–1150 cm^{-1} zone.

Another difference concerns the band at 982 cm^{-1}, only observed in the spectra of the cellular

preparations exposed to SYN as shown in the enlargement of the 1020–940 cm^{-1} zone (Figure 6). Since this band is not detected in the spectra of the associated buffers, it can be logically ascribed to a specific answer of components present in the cell lysate when exposed to SYN. It is noteworthy that this band is more intense in the SYN than in the SYN+URG7 cellular preparation. In literature data this band is widely attributed to the specific absorption of RNA (uracyl ring motion) [25,26].

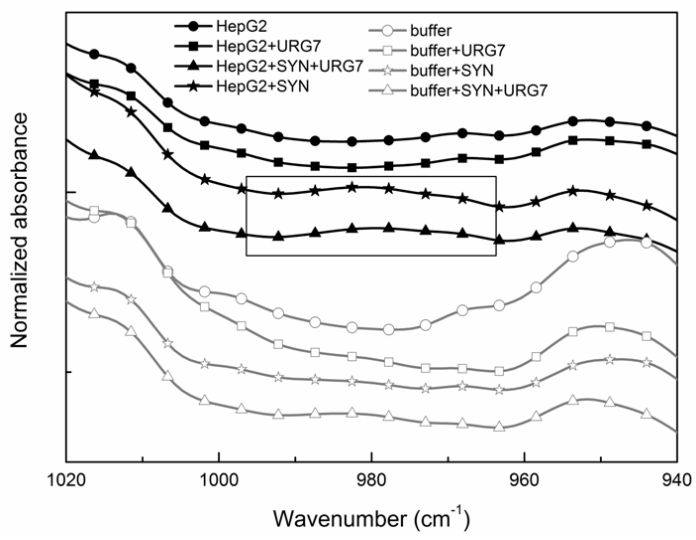

Figure 6. Raw FTIR spectra of cellular dried films and buffer preparations in the 1200–940 cm^{-1} zone.

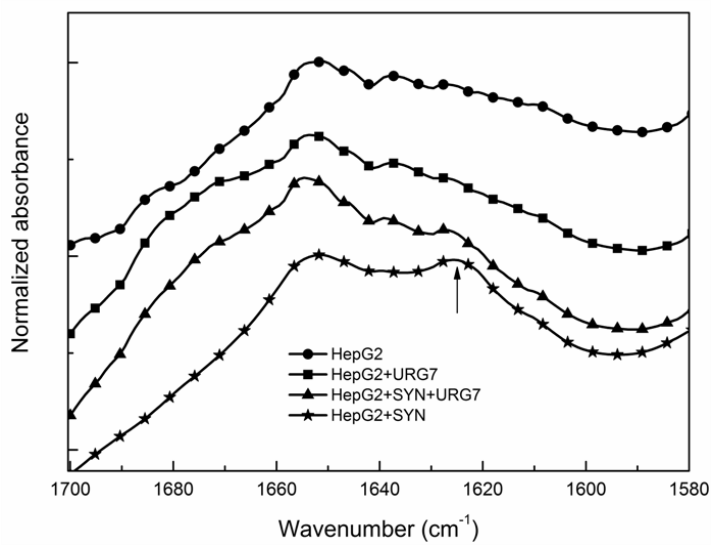

Figure 7. Raw FTIR spectra of cellular dried films in the 1700–1580 cm^{-1} zone.

Finally, the shape of the Amide I, well-known to be sensitive to secondary structures of proteins, is strongly modified in cellular preparation exposed to SYN with the intensification of the 1625 cm^{-1} band associated with intra molecular β-sheets and widely attributed to protein aggregation [27,28] as

shown on Figure 7 (arrow).

This peculiar intensification of the 1625 cm^{-1} component is not observed in cellular preparation exposed to SYN and subsequently treated by URG7. This fact is confirmed by the comparison of the FSD spectra (Figure S1, Supplementary material).

The decomposed FTIR spectra of the four cellular preparations are reported on Figure S2 (Supplementary material). The location of the different peak components and their probable assignment according to literature data [24,27–29] are reported on Table 2, showing the multiplicity of protein secondary structures present in these cellular preparations.

Table 2. Location of the peaks from the fitting procedure of Amide I and probable assignment.

Band position (cm^{-1})	**Assignment**
1694	anti-parallel β sheets and turns
1685	β turns and β sheets
1673	PPII, turns, loops
1664	Turns, loops
1654	Helices/random coil
1646	Random coils/water
1637	Intra molecular β sheets
1625	Inter molecular β sheets = cross β structures
1609	Side chain (Gln)

The ratio area of each peak was computed and reported in Figure S3 (Supplementary material). We chose to present in Figure 7 the ratio corresponding to the 1625 cm^{-1} component ascribed to intermolecular β-sheets, signature of aggregated proteins into cross-β structures [27,28].

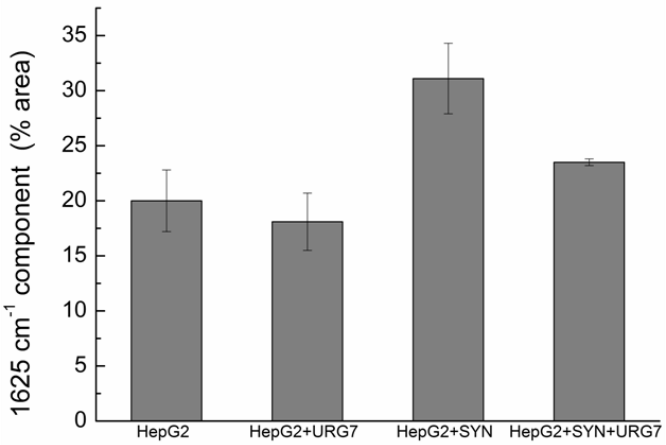

Figure 8. Evolution of the protein's secondary structures. Mean with standard deviation of the area ratio for the 1625 cm^{-1} component (N = 3).

This diagram clearly evidences the evolution of the protein's secondary structures in the different cellular preparations: the amount of cross-β structures is similar both in HepG2 cell lysate and HepG2 cell lysate treated with URG7-peptide. It significantly increases in HepG2 cells lysate incubated with SYN while it decreases to an intermediate value when cell lysates are incubated with SYN and subsequently treated by URG7.

4. Discussion

URG7, a protein transactivated by the hepatitis B antigen X, acts as a reliever of ER stress-induced apoptosis by decreasing the amount of unfolded proteins [7,8]. In this study *in vitro* experiments monitored by differential scanning calorimetry and FTIR-ATR were carried out to evaluate the potential of URG7 and the specific peptide 75–99 URG7-peptide [9] as a protein folding modifier on HepG2 cell lysates and on α-synuclein, one of the main protein responsible for neurogenerative diseases. When HepG2 cells are treated with tunicamycin, their expression level of Endoplasmic Reticulum stress markers was twofold higher compared to untreated cells and their folding ability in stress increased [8]. Folding and unfolding processes (strongly dependent on the peculiar environment where they take place) are the ways to generate or abolish cellular activity [30]. Hence, considering interfacial water behavior is valuable.

Our objective was to check if these biochemical changes driven modifications on the thermodynamics of cells suspensions in water. The DSC scans demonstrated that in the [−30, 10 ℃], there are two-phase transitions: the eutectic melting (at about −20 ℃) superimposed on the continuous melting of freezable bound water, also designed as interfacial water and assigned to mobile water since its melts below 0 ℃ [21].

4.1. URG7 transfection

In URG7-transfected cells, we noted a shift toward low temperature of the eutectic melting. This destabilization of mobile water in the eutectic phase corresponds to an easier reorientation of the system water molecules-salt surrounding the surface of protein. Moreover, the decrease of enthalpy generated by the tunicamycin was attenuated, demonstrating that the water molecules at the external surface of cell lysate were significantly perturbed by URG7 transfection. In URG7 transfected HepG2 cells, a modification of misfolded proteins and the production of two distinct protein products which one was sensitive to tunicamycin treatment were evidenced [8]. This behavior could be correlated to the peculiar response occurred in stressed URG7 transfected cells. The orientation ability of interfacial hydration was modified compared to HepG2 cells and a large increase of eutectic melting enthalpy suggested an important mobile fraction water. In stressed transfected cells, URG7 acted to an "anti-freezing" agent driving to an evolution of hydration shell. This behavior could be correlated to the decrease of endoplasmic reticulum stress, and the attenuation of protein folding ability observed by Armentano et al. [8].

4.2. URG7 peptide treatment

Biophysical characterization showed that in all solvents URG7 peptide contains secondary structures, and possesses 50% of hydrophobic residues which decrease its solubility in polar solvents.

Far UV CD experiments evidenced a heterogeneous population of α-helix and β-structure in physiological conditions [4]. Among hydrophobic aromatic amino acids, in particular tryptophan residues contributed to stabilize the α-helix [31], conferring a strong stability to the polypeptide.

To obtain a global view on interfacial water around the lysated samples, the amount of mobile water in low temperature was evaluated (Figures S4, S5, Supplementary material) following the method described and validated by Kamasa et al. [16], and Tompa et al. [21].

In cell lysates, we can observe the thermal effect on eutectic melting and melting of primary ice for each added product. As shown in Figure S4 (Supplementary material), we can also evidence an important fraction of mobile water below 0 ℃. Tunicamycin induced an increase of stability of mobile water, abolished by URG7 in the case of combined treatment, and a decrease of eutectic enthalpy melting. The increase of stability promoted by tunicamycin was not observed in cells, showing the peculiar cellular response in stress conditions. At around −20 ℃, the mobile fraction water decreased strongly with tunicamycin. In stress conditions URG7 was able to maintain the same fraction of mobile water that untreated cells. URG7 was able to restore the water reorientation ability around the complex lysate system. DSC results confirm through the interfacial water behavior that URG7 is able to act in two ways: it maintains the interfacial water stability and controls the mobile fraction level, associated with the peculiar folding of this biological system.

With its peculiar ability to maintain cells stability and to inhibit the modification of mobile fraction water, URG7 potential was also faced to synuclein, responsible for degenerative diseases.

As evidenced in Figure S5 (Supplementary material), the mobile water phase increases strongly for cells exposed to SYN at about −20 ℃, demonstrating an important influence on water hydration. URG7 peptide treatment tends to restore water hydration. FTIR results evidenced an increase of 31% of cross β structure in cells exposed to synuclein, associated with aggregated proteins. Cremades et al. [10] reported the conversion of α-synuclein from disordered monomeric state to fibrillar state rich in cross β structures. In super cooling conditions, a cold denaturation of amyloid fibrils, named disaggregation, can be detected by NMR at −15 ℃ with the collapse of long-range interactions [11,32,33]. Following cold denaturation, the structures of oligomers are intermediate between those of monomers and fibrils and are able to disrupt lipid membranes [33,10]. Our calorimetric results in this range of temperature evidenced an important mobile hydration shell reaching 10%. With URG7-peptide this hydration shell decreased to 5%, and FTIR evidenced only 23% of cross β structure. The peculiar sequence and shape of URG7 could be responsible for the large decrease of cross β structures. It maintains the interfacial fraction water around cell lysates samples and inhibits the reorientation of mobile fraction water induced by synuclein.

Recent studies underlined the importance of the central region of synuclein, named NAC domain, highly hydrophobic and responsible for the ability to undergo a conformational change from random coil to β-sheet. Fusco et al. assume this domain regulates the affinity of α-synuclein for cell membranes [34]. Carija et al. [35] validated the important role of the NAC domain in the α-synuclein aggregation. They chemically built a more compact conformation that impacted drastically the aggregation behavior. These authors hypothesized that limiting the exposure of NAC domain in soluble α-synuclein could be a good strategy to inhibit aggregation.

DSC results shed light on mobile water hydration of protein lysates of cells treated or transfected with URG7 in stressed conditions. URG7 acted to maintain the hydration shell surrounding the complex structure and FTIR brought to the fore an important decrease of the cross β-structures in sample treated with URG7 in presence of synuclein. These different markers confirmed that URG7

maintained the structural conformation of the complex structure and inhibited the cross β formation.

The comparable behavior observed for the interaction between URG7-peptide and α-synuclein in the presence of the cell extract compared to experiments with only peptides suggest that the URG7 does not act alone but require other cellular components.

Conclusions

Differential scanning calorimetry and FTIR allowed us to highlight an intrinsic property of URG7 which is to modify the aggregation state of the proteins present in stressed cells lysates. The property of URG7 as a stress attenuator is also confirmed in the experiments with α-synuclein thus suggesting its possible use in the pharmacological treatment of neurogenerative diseases.

Conflict of interest

The author declares no conflict of interest.

References

1. Lian Z, Liu J, Pan J, et al. (2001) A cellular gene up-regulated by hepatitis B virus-encoded X antigen promotes hepatocellular growth and survival. *Hepatology* 34: 146–157.
2. Ostuni A, Lara P, Armentano MF, et al. (2013) The hepatitis B x antigen anti-apoptotic effector URG7 is localized to the endoplasmic reticulum membrane. *FEBS Lett* 587: 3058–3062.
3. Lee H, Lara P, Ostuni A, et al. (2014) Live-cell topology assessment of URG7, MRP6102 and SP-C using glycosylatable green fluorescent protein in mammalian cells. *Biochem Biophys Res Commun* 450: 1587–1592.
4. Ostuni A, Antonietta Castiglione Morelli M, Miglionico R, et al. (2014) Expression, purification and structural characterization of Up-regulated gene 7 encoded protein. *Protein Peptide Lett* 21: 413–418.
5. Hayer J, Jadeau F, Del éage G, et al. (2013) HBVdb: a knowledge database for hepatitis B virus. *Nucleic Acids Res* 41: 566–570.
6. Pan J, Lian Z, Wallett S, et al. (2007) The hepatitis B x antigen effector, URG7, blocks tumour necrosis factor alpha-mediated apoptosis by activation of phosphoinositol 3-kinase and beta-catenin. *J Gen Virol* 88: 3275–3285.
7. Li B, Gao B, Ye L, et al. (2007) Hepatitis B virus X protein (HBx) activates ATF6 and IRE1-XBP1pathways of unfolded protein response. *Virus Res* 124: 44–49.
8. Armentano MF, Caterino M, Miglionico R, et al. (2018) New insights on the functional role of URG7 in the cellular response to ER stress. *Biol Cell* 110: 147–158.
9. Ostuni A, Bisaccia F (2019) Method for diagnosing the risk of preneoplastic and neoplastic liver disease in subjects affected by hepatitis. *European Patent EP3161488A1*.
10. Cremades N, Chen SW, Dobson CM (2017) Structural characteristics of alpha-synuclein oligomers. *Int Rev Cell Mol Biol* 329: 79–143.
11. Kim HY, Heise H, Fernandez CO, et al. (2007) Correlation of amyloid fibril Beta- structure with the unfolded state of alpha-synuclein. *Chembiochem* 8: 1671–1674.
12. Uversky VN, Elieser D (2009) Biophysics of Parkinson's desease: Structure and aggregation of alpha-synuclein. *Curr Protein Peptide Sci* 10: 483–499.

13. Johnson CM (2013) Differential scanning calorimetry as a tool for protein folding and stability. *Arch Biochem Biophys* 531: 100–109.
14. Briere LA, Brandt JM, Medley J (2010) Measurement of protein denaturation in human synovial fluid and its analogs using differential scanning calorimetry. *J Therm Anal Calorim* 102: 99–106.
15. Lunetti P, Cappello AR, Marsano RM, et al. (2013) Mitochondrial glutamate carriers from Drosophila melanogaster: biochemical, evolutionary and modeling studies. *BBA-Bioenergetics* 1827: 1245–1255.
16. Kamasa P, Bokor M, Pyda M, et al. (2007) DSC approach for the investigation of mobile water fractions in aqueous solutions of NaCl and Tris buffer. *Thermochimica Acta* 464: 29–34.
17. Ostuni A, Miglionico R, Castiglione Morelli MA, et al. (2010) Study of the nucleotide-binding domain 1 of the human transporter protein MRP6. *Protein Peptide Lett* 17: 1553–1558.
18. Salvia AM, Cuviello F, Coluzzi S, et al. (2017) Expression of some ATP-binding cassette transporters in acute myeloid leukemia. *Hematol Rep* 9: 137–141.
19. Miglionico R, Ostuni A, Armentano MF, et al. (2017) ABCC6 knockdown in HepG2 cells induces a senescent-like cell phenotype. *Cell Mol Biol Lett* 22: 7.
20. Martinelli F, Cuviello F, Pace MC, et al. (2018) Extracellular ATP regulates CD73 and ABCC6 expression in HepG2 cells. *Front Mol Biosci* 5: 75.
21. Tompa K, Bánki P, Bokor M, et al. (2009) Interfacial water at protein surfaces: Wide-line NMR and DSC characterization of hydration in ubiquitin solutions. *Biophys J* 96: 2789–2798.
22. Dandurand J, Samouillan V, Lacabanne C, et al. (2015) Water structure and elastin-like peptide aggregation. *J Therm Anal Calorim* 120: 416–426.
23. Mehra S, Sahay S, Maji SK (2019) Alpha synuclein misfolding and aggregation: Implications in Parkinson's disease pathogenesis. *BBA- Proteins Proteonomics* 1867: 890–908.
24. Staniszewska E, Malek K, Baranska M (2014) Rapid approach to analyze biochemical variation in rat organs by ATR FTIR spectroscopy. *Spectrochim Acta-Part A Mol Biomol Spectrosc* 118: 981–986.
25. Ami D, Neri T, Natalello A, et al. (2008) Embryonic stem cell differentiation studied by FT-IR spectroscopy. *BBA-Mol Cell Res* 1783: 98–106.
26. Wood BR (2016) The importance of hydration and DNA conformation in interpreting infrared spectra of cells and tissues. *Chem Soc Rev* 45: 1980–1998.
27. Bochicchio B, Pepe A, Crudele M, et al. (2015) Tuning self-assembly in elastin-derived peptides. *Soft Matter* 11: 3385–3395.
28. Litvinov RI, Faizullin DA, Zuev YF, et al. (2012) The a-helix to b-sheet transition in stretched and compressed hydrated fibrin clots. *Biophys J* 103: 1020–1027.
29. Barth A (2007) Infrared spectroscopy of proteins. *BBA-Bioenergetics* 1767: 1073–1101.
30. Dobson CM (2003) Protein folding and misfolding. *Nature* 426: 884–890.
31. De Planque MRR, Killian JA (2003) Protein–lipid interactions studied with designed transmembrane peptides: role of hydrophobic matching and interfacial anchoring. *Mol Membr Biol* 20: 271–284.
32. Kim HY, Cho MK, Riedel D, et al. (2008) Dissociation of amyloid fibrils of α-synuclein in supercooled water. *Angew Chem Int Edit* 120: 5124–5126.
33. Kim HY, Cho MK, Kumar A, et al. (2009) Structural properties of pore-forming oligomers of α-Synuclein. *J Am Chem Soc* 131: 17482–17489.

34. Fusco G, De Simone A, Gopinath T, et al. (2014) Direct observation of the three regions in α-synuclein that determine its membrane-bound behaviour. *Nat Commun* 5: 3827.
35. Carija A, Pinheiro F, Pujols J, et al. (2019) Biasing the native α-synuclein conformational ensemble towards compact states abolishes aggregation and neurotoxicity. *Redox Biol* 22: 101135.

AIMS Press